

MODELING UNCERTAINTIES IN A CRACKED ROD MODELED WITH THE SPECTRAL ELEMENT METHOD

Fabro, A.T., adrianotf@fem.unicamp.br

Computational Mechanics Department, University of Campinas, CEP 13083-970, Campinas, SP, Brazil

Ritto, T.G., thiagoritto@gmail.com

Sampaio, R., rsampaio@puc-rio.br

Mechanical Engineering Department - PUC-Rio, CEP 22453-900, Rio de Janeiro, RJ, Brazil

Arruda, J.R.F., arruda@fem.unicamp.br

Computational Mechanics Department, University of Campinas, CEP 13083-970, Campinas, SP, Brazil

Abstract. *The aim of this paper is to quantify the probability of failure of a cracked rod considering a stochastic dynamic model for a proposed probabilistic model. Uncertainties must be taken into account for a robust analysis and to increase the predictability of the model. The cracked rod is modeled with the spectral element method and the flexibility of the crack is considered uncertain. To model the uncertainties, the parametric probability approach is employed and the Maximum Entropy Principle is used to derive the probability density function. Then, a reliability analysis is done and the probability of failure is calculated for different failure surfaces, using Monte Carlo sampling.*

Keywords: *Dynamical system, Wave propagation, Uncertainty quantification, Stochastic analysis, Reliability analysis.*

1. INTRODUCTION

The aim of this work is to quantify the probability of failure of a damaged structure for a proposed probabilistic model. Specifically, a cracked rod is considered. Probability theory is used to model the uncertainties of the problem and a criterion is established to characterize the failure. Monte Carlo sampling is used as the stochastic solver. In this analysis only the flexibility of the crack is considered uncertain. The Maximum Entropy Principle (Jaynes, 1957a,b; Shannon, 1948) is used to derive the probability density function of the random variable related to the flexibility of the crack. Using this principle it is assured that the realizations of the random variable are compatible with the physics of the problem. A failure happens when the Damage Index (DI) (which is defined in Section 3) is greater than a prescribed limit, a failure surface. A reliability analysis is performed in order to assess the robustness of the given crack model. The prescribed limit for the DI is increased until no failure occur.

Most of the existing monitoring methods are local and presume that the location of the damage is known and the damage area is readily accessible. Vibration-based methods and wave propagation methods provide tools for global structural monitoring including parts that are either inaccessible or difficult to make measurements on (Ostachowicz, 2008). Small defects such as cracks are obscured by modal approaches because such phenomena have a local nature and only affect significantly the high frequency behavior. Wave propagation-based structural models are well suited for detecting this kind of defect since they are sensitive to changes in the local dynamic impedance (Palacz and Krawczuk, 2002) and it is known that material discontinuities affect the propagation of elastic waves in solids (Ostachowicz, 2008). Frequencies that are most sensitive to damage depend on the type of structure, the type of material, and the type of damage (Ostachowicz, 2008; Palacz and Krawczuk, 2002). Among the wave propagation methods, the Spectral Element Method (SEM) allows to combine the analytical approach with the matrix approach of the Finite Element Method (FEM), with a fundamental difference that the element stiffness matrix is established in the frequency domain (Doyle, 1997).

This article is organized as follows. In Section 2. the model of the cracked rod is presented and a DI is defined in Section 3. Then, in Section 4. the probabilistic model for the flexibility of the crack is developed and the reliability analysis is presented in Section 5. Numerical results are discussed in Section 6.. Finally, in Section 7. the concluding remarks are presented.

2. SPECTRAL CRACKED AND NON-CRACKED ROD FINITE ELEMENT

There are different ways of establishing a dynamic stiffness relationship. In fact, the SEM approach does it via dynamic shape function which use the exact displacement distributions as the interpolation function between the element ends (Doyle, 1997). The SEM is formulated based on two types of elements: two-noded and throw-off. The latter are used when the member extends to infinity. The major drawback of SEM is that the elements may only be assembled in one dimension. The solution along the orthogonal dimensions has to be found analytically and it is only possible for simple geometries (Arruda et al., 2007).

2.1 Two-Noded Spectral Rod Finite Element.

It uses the most simple rod theory. A spectral element of length L and the end displacements as boundary conditions, the following symmetric dynamic stiffness element matrix can be obtained (Doyle, 1997):

$$[K] = \frac{iEAk}{1-z^2} \begin{bmatrix} 1+z^2 & -2z \\ -2z & 1+z^2 \end{bmatrix}, \quad (1)$$

where $z = e^{-ikL}$, k is the wave number defined by $k = 2\pi f_k \sqrt{\rho/E}$ with f_k being the discretized frequency, A is the cross section area, ρ the mass density, and E the Young's modulus. With the dynamic stiffness matrix of an element, it is straightforward to assemble a global stiffness matrix using the direct stiffness method (Craig, 1981). The structural responses can be found by solving, for each frequency, a linear system of equations of the type $\hat{\mathbf{F}} = [K]\hat{\mathbf{U}}$, where $[K]$ is the complex dynamic stiffness matrix for the rod element, $\hat{\mathbf{F}}$ is the vector of complex amplitudes of the nodal forces, and $\hat{\mathbf{U}}$ is the vector of the complex nodal displacement amplitudes. In order to account for structural damping, an internal loss factor η can be applied by using a complex Young's modulus $E(1+i\eta)$.

2.2 Spectral Rod Throw-off Element.

The dynamic stiffness for the throw-off element is given by (Doyle, 1997):

$$K_t = iEAk. \quad (2)$$

This implies that the system experiences dissipation, since the throw-off element conducts energy out of the system.

2.3 Spectral Cracked Rod Finite Element.

A spectral rod finite element with a transverse open and non-propagating crack was presented by Palacz and Krawczuk (2002). The length of the element is L , and its area of cross-section is A . The crack, located at L_1 , is substituted by a dimensionless spring, whose flexibility θ is calculated by using Castigliano's theorem and the laws of the fracture mechanics.

The dynamic stiffness matrix for the spectral cracked rod element is given by :

$$[K_c] = iEAk \begin{bmatrix} [D]_{11}^{-1} - [D]_{21}^{-1} z_1 & [D]_{14}^{-1} - [D]_{24}^{-1} z_1 \\ -[D]_{31}^{-1} z + [D]_{41}^{-1} & -[D]_{34}^{-1} z + [D]_{44}^{-1} \end{bmatrix}, \quad (3)$$

where $z_1 = e^{-ikL_1}$ and $[D]_{ij}^{-1}$ denotes the element ij of the inverse of matrix $[D]$, which takes into account the nodal spectral displacements for the left and right part of the rod and the boundary conditions:

$$[D] = \begin{bmatrix} 1 & z_1 & 0 & 0 \\ (ik\theta - 1)z_1 & (-1 - ik\theta) & z_1 & zz_1^{-1} \\ -ikz_1 & ik & ikz_1 & -ikzz_1^{-1} \\ 0 & 0 & z & 1 \end{bmatrix}. \quad (4)$$

The dimensionless form of the flexibility is expressed as (Ostachowicz, 2008; Palacz and Krawczuk, 2002; Krawczuk et al., 2006a,b):

$$\theta = 2\pi h \int_0^{\bar{\alpha}} \bar{\alpha} g^2(\bar{\alpha}) d\bar{\alpha}. \quad (5)$$

where $\bar{\alpha} = a/h$ show the ratio between depth crack and height of cross section height h , and g is a correction function defined by

$$g\left(\frac{\alpha}{h}\right) = \sqrt{\frac{\tan(\pi\alpha/2h)}{\pi\alpha/2h}} \times \frac{0.752 + 2.02(\alpha/h) + 0.37(1 - \sin(\pi\alpha/2h))^3}{\cos(\pi\alpha/2h)}. \quad (6)$$

2.4 Clamped Semi-Infinite Rod Modeling.

The assembling of the global dynamic stiffness matrix uses the same procedure as the usual FEM approach but it is evaluated at each frequency component of the analysis. Assembling the structural stiffness matrix (Doyle, 1997; Craig, 1981), using Eq. 1 and Eq. 2, and applying the clamped constraint, we have:

$$K_G = [K]_{22} + K_t = \frac{iEAk}{1-z^2}(1+z^2) + iEAk = \frac{i2EAk}{1-z^2}, \quad (7)$$

where $[K]_{22}$ is the element at the second line and second column of $[K]$ (see Eq. 1). With the same procedure, using the spectral cracked rod element, Eq. 3, together with the throw-off element, Eq. 2, and applying the clamped constraint, yields:

$$K_{Gc} = [K_c]_{22} + K_t = iEAk(-[D]_{34}^{-1}z + [D]_{44}^{-1}) + iEAk = iEAk(1 - [D]_{34}^{-1}z + [D]_{44}^{-1}). \quad (8)$$

Figure 2.4 shows the clamped semi-infinity cracked rod and the cross-section of the rod element at the crack location.

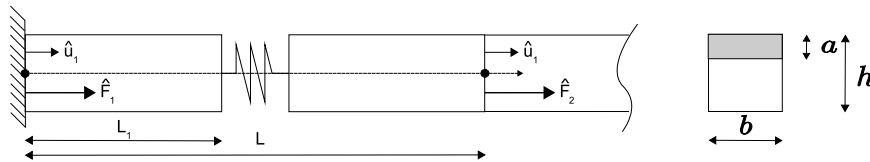


Figure 1. Dimensions of the cracked rod considered.

3. DAMAGE INDEX

A damage index (DI) is used to compare the difference between the dynamic responses of the cracked and non-cracked rod. The DI used is defined as follows (Banerjee et al., 2009):

$$DI = \left| 1 - \frac{\sum_{f_k=0}^{f_s/2} FD^2(f_k)}{\sum_{f_k=0}^{f_s/2} FI^2(f_k)} \right|, \quad (9)$$

where $FD(f_k)$ and $FI(f_k)$ are the magnitudes of the frequency response functions or spectra for the damaged and undamaged structure, evaluated at frequency f_k , respectively, and f_s is the sampling rate. If the structure is undamaged, $DI = 0$. Using the dynamic stiffness, defined by Eq. 7 and Eq. 8, with an input excitation \hat{F} , Eq. 9 becomes:

$$DI = \left| 1 - \frac{\sum_{f_k=0}^{f_s/2} |(K_{Gc}(f_k))^{-1} \hat{F}(f_k)|^2}{\sum_{f_k=0}^{f_s/2} |(K_G(f_k))^{-1} \hat{F}(f_k)|^2} \right| = \left| 1 - \frac{\sum_{f_k=0}^{f_s/2} |(iEAk(1 - [D]_{34}^{-1}z + [D]_{44}^{-1}))^{-1} \hat{F}(f_k)|^2}{\sum_{f_k=0}^{f_s/2} |(i2EAk)^{-1} \hat{F}(f_k)|^2} \right|. \quad (10)$$

Note that the DI is strongly dependent of the input excitation \hat{F} , what means the this DI can not be used as an absolute measure of damage. Using the initial measurements performed on an undamaged structure as baseline, damage indexes are evaluated from the comparison of the frequency response of the monitored structure with an unknown damage.

4. PROBABILISTIC MODELING

The probability theory is used to model the uncertainties of the problem. For this analysis, it is considered that the crack location is known, but its severity is unknown. Therefore, we consider the value of the crack flexibility θ , which is a measure of the damage severity, uncertain. And it is the only uncertainty taken into account in the present analysis. Note that θ depends on the rod height h and on the crack depth a (see Eq. 5). But instead of constructing a probabilistic model for h and a , we construct it directly to our variable of interest, θ . This is a new approach for the problem. The advantage of this approach is that it allows the construction of a general probabilistic model that describes well most practical problems.

To construct the probability density function (PDF) of the random variable related to the flexibility of the crack, Θ , the Maximum Entropy Principle is used (Jaynes, 1957a,b; Shannon, 1948). The idea is to use the information we have

about the random variable, so that the distribution used for the random variable chosen is compatible with the physics of the problem.

The first available information we have is that the mean value of the random variable Θ is known. This is because we trust the mean model, so (see Eq. 5):

$$\mathbb{E}\{\Theta\} = \underline{\theta}, \quad (11)$$

where $\underline{\theta}$ is calculated using the nominal values of the variables in Eq. 5 and $\mathbb{E}\{\cdot\}$ is the mathematical expectation. The second available information we have is that the value of the flexibility is always positive, *i.e.*,

$$\Theta \in]0, +\infty[. \quad (12)$$

The third available information is:

$$\mathbb{E}\{\ln(\Theta)\} = |\text{cte}| < +\infty. \quad (13)$$

This is because the probability should go to zero as Θ approaches zero, otherwise there could exist a local stiffness going to infinity what is not reasonable. The optimization problem is given by:

$$\underset{f_{\Theta}(\theta)}{\text{maximize}} \quad S(f_{\Theta}(\theta)), \quad (14)$$

subjected to Eq. 11, Eq. 12, and Eq. 13, where the entropy measure is given by :

$$S(f_{\Theta}(\theta)) = - \int_0^{+\infty} f_{\Theta}(\theta) \ln(f_{\Theta}(\theta)) d\theta. \quad (15)$$

The probability density function found for Θ is the Gamma density function (Kapur and Kesavan, 1992) given by:

$$f_{\Theta}(\theta) = \mathbb{1}_{]0, +\infty[}(\theta) \theta^{a_0-1} \frac{\exp(-\theta/b_0)}{b_0^{a_0} \Gamma(a_0)}, \quad (16)$$

where $\mathbb{1}_B(\theta)$ is an indicator function that is equal to 1 for $\theta \in B$ and 0 otherwise, and $\Gamma(z) = \int_0^{+\infty} t^{z-1} e^{-t} dt$ is the Gamma function defined for $z > 0$. The parameters of the distributions are given by $a_0 = 1/\delta_{\Theta}^2$ and $b_0 = \underline{\theta}/\delta_{\Theta}^2$. The generation of a random variable that follows a Gamma distribution is implemented in many computer codes.

5. RELIABILITY ANALYSIS

Reliability Analysis aims to evaluate the probability of failure, *i.e.*, the probability that the system response does not satisfy a performance criterion. In (Schuëller, 2007) a rational treatment of uncertainties in structural mechanics and analysis is presented, in (Schuëller, 2001) some developments of computational stochastic mechanics and analysis are reviewed. The system under analysis takes into account randomness (see Section 4) and a performance, or failure, criterion is defined using a *DI* (see Section 3). It should be noted that if there is more than one failure criterion, each of them needs a different reliability analysis.

The functional relationship between the performance criterion and the random variables can be expressed as a performance function (Haldar and Mahadevan, 2000), as follows:

$$Z = g(\mathbf{X}), \quad (17)$$

where \mathbf{X} is the random vector composed by the random variables of the problem. The failure surface or the limit state is defined by $Z = 0$, and the failure occurs when $Z < 0$. The probability of failure is given by (Haldar and Mahadevan, 2000; Rackwitz, 1991; Sudret and der Kiureghian, 2000):

$$PF(\mathbf{X}) = \int_{g < 0} f_{\mathbf{X}}(\mathbf{x}) d\mathbf{x}, \quad (18)$$

in which $f_{\mathbf{X}}$ is the PDF of the random variable \mathbf{X} , and the domain of integration is defined by the set $g < 0 = \{\mathbf{x} : g(\mathbf{x}) < 0\}$. To evaluate the integration in Eq. 18 is equivalent to calculate the probability of failure of the system under analysis. In general, the PDF is almost impossible to obtain and even if it were known, the integration above would not be easily calculated (Haldar and Mahadevan, 2000). The standard Monte Carlo Method is a non-intrusive and well-suited method to calculate the failure probability. It is calculated from the sum of N realizations of the random variable \mathbf{X} for which a failure occurs among N runs, as follows:

$$\hat{PF} = \frac{1}{N} \sum_{i=1}^N \mathbb{1}_{g < 0}(\mathbf{X}_i), \quad (19)$$

where \hat{PF} is an unbiased estimator of $PF(\mathbf{X})$, Eq. 18. Eq. 19 means that the probability of failure can be estimated as a ratio of the number of runs that lead to failure, n_f , and the total number of the runs performed, $\hat{PF} = n_f/N$. By the Central Limit theorem, \hat{PF} has approximately a normal distribution $N(PF, N^{-1}Var(PF))$ for large N , where $Var(PF)$ can be estimated via the sample variance unbiased estimator, $S^2 = (1/(N - 1)) \sum_{i=1}^N (PF_i - \hat{PF})^2$, with which we can estimate a confidence interval (Rubinstein and Kroese, 2008). The disadvantage of the direct Monte Carlo sampling is that when PF is small a very big number of simulations may be necessary for convergence. For instance, if $PF = 10^{-3}$ it is necessary an average of 1000 simulations for a failure to happen.

6. NUMERICAL RESULTS

6.1 Deterministic response.

For the numerical tests, we consider a semi-infinity clamped rod, as shown in Fig. 2.4n which $L = 4$ m, $L_1 = 2.4$ m, $b = 0.02$ m, $h = 0.02$ m, $E = 210$ GPa, $\rho = 7850$ kg/m³, and $\eta = 0.001$. A pulse is applied at $x = L$ from the clamped node and the crack is at $x = L_1$. Eq. 7 shows the dynamic stiffness used to model the healthy rod and Eq. 8 was used to model the dynamic stiffness of the cracked rod. We consider the crack with depth equal to $\bar{\alpha} = 0.15$ of the height of the rod and Eq. 5 is used to calculate the dimensionless form for the local flexibility, θ .

The analysis was carried out for two different bursts, that were constructed using a sine function with frequency 80 kHz and 100 kHz with 10 N of amplitude. It is important to apply a suitable windowing in order to obtain a narrowband burst. This is important for the damage detection processes, when the measured data is usually polluted with broadband noise. The triangular window is built with 10 sine periods width, for each excitation frequency, and results are show at Fig. 2(a) and Fig. 2(b).

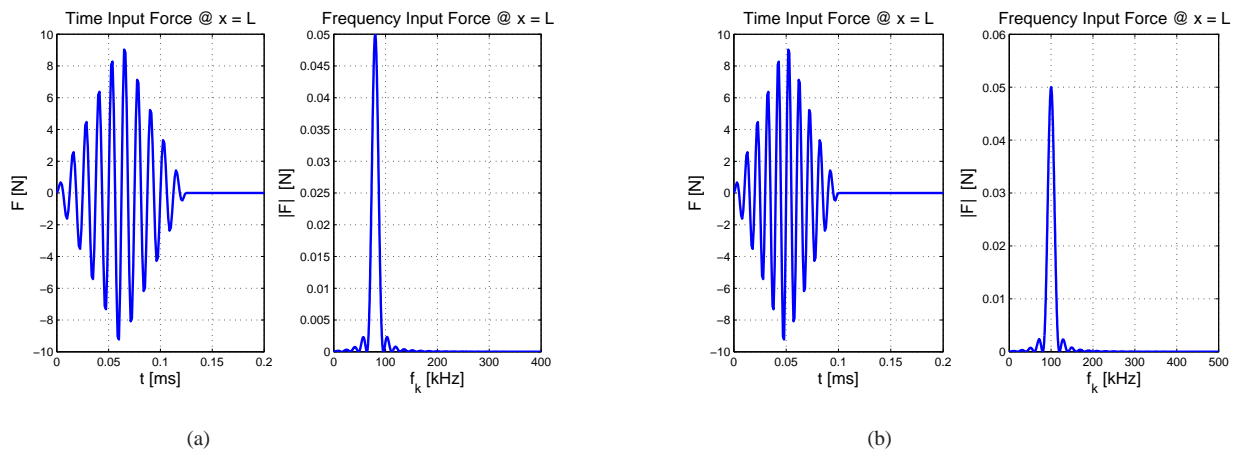
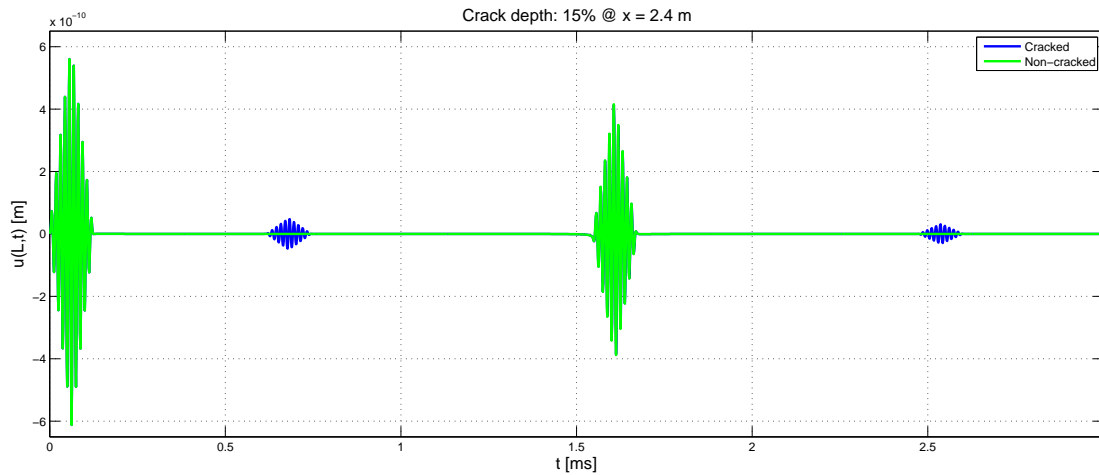


Figure 2. Mean Model. Applied input force for a damage and undamaged rod. (a) 80 kHz (b) 100 kHz.

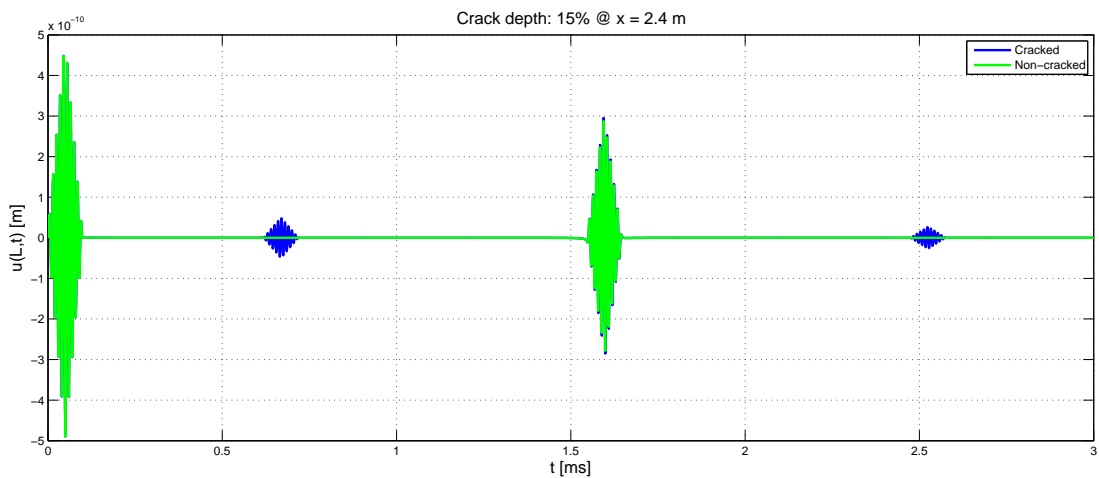
Figure 3(a) and Fig. 3(b) show the time response at $x = L$, the same location of the excitation burst, for the damage and the undamaged rod. Note that the first 0.1 ms the rod response while the burst is being applied, so they are the same for the damaged and undamaged rod.

The applied excitation creates longitudinal propagation waves. For the healthy rod, this burst travels over the structure and it is observed again at $t = (2 \times L)/C_v = 1.55$ ms, where C_v is the velocity of propagation of the wave, and after it is dissipated at its infinity side, modeled by the throw-off element, Eq. 2, conducting energy out of the system. Note that its amplitude is smaller only due to the structural damping, η . Otherwise, for the damaged rod, note that Fig. 3(a) and Fig. 3(b) show two more bursts, related to the crack. When the propagating wave reaches the crack location, it is

partly transmitted and partly reflected, due to the abrupt change at the local flexibility. If there is no crack, all the energy is transmitted over and no wave is reflected. The larger the crack depth the less energy will be transmitted across the crack location. Then, the crack depth establish the amplitude of the reflected and transmitted wave. Note that the first reflection is at $t = 2 \times (L - L_1)/C_v = 0.6$ ms. The wave that was transmitted across the crack reaches the clamped side and then it is totally reflected. This is observed at $t = (2 \times L + 2 \times L_1)/C_v = 2.5$ ms. After it is dissipated at its infinity side. Eq. 10 was used to calculate the damage index, for $\bar{a} = 0.15$, being $DI = 0.0014$ for 100 kHz and $DI = 0.0006$ for 80 kHz for the depth crack.



(a)



(b)

Figure 3. Mean Model. Time response for the damaged and undamaged rod for the different excitations: (a) 80 kHz and (b) 100 kHz.

Figure 4 shows the influence of the crack depth at DI for the different frequency excitation, using ten periods. Note that for the 100 kHz excitation the DI has a bigger sensibility to the crack depth, what is reasonable because the bigger the frequency of the wave traveling over the rod the smaller its wavelength, and the bigger its sensibility to small defects. For frequency excitations bigger than 100 kHz, high order rod theories are required (Doyle, 1997). Spectral Cracked Rod Finite Element for higher order rod theories can be found at Krawczuk et al. (2006a,b) and Pereira (2009).

6.2 Reliability analysis.

A $\bar{a} = 0.15$ crack depth and $h = 0.02$ m were used in Eq. 5 to compute $\underline{\theta}$. Fig. 5(a), Fig. 5(b) and Fig. 5(c) show histograms built using 20,000 MC simulation for three different values of the coefficient of variation, $\delta_{\Theta} = 0.05$, $\delta_{\Theta} = 0.1$ and $\delta_{\Theta} = 0.2$, respectively, using burst shown at Fig. 2(b). DI for nominal model, Eq. 11, is shown in green and DI for estimated mean is shown in red. Tab. 1 summarize this results.

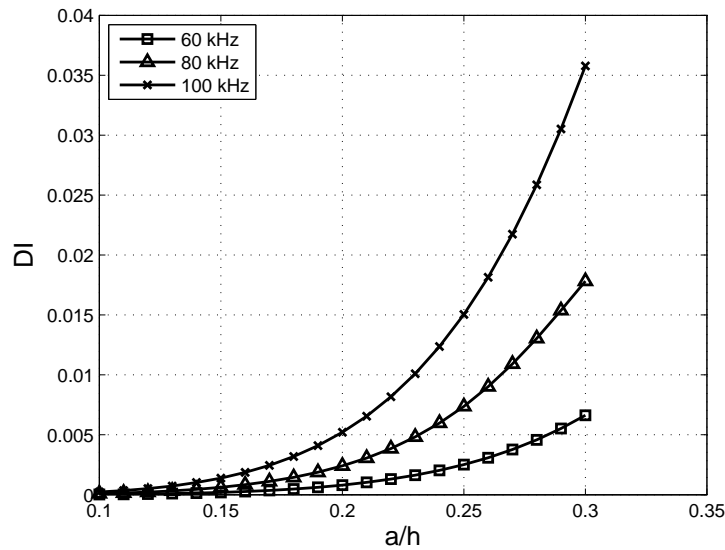


Figure 4. Sensibility of DI for different crack depth and frequency excitation.

	$\delta_{\Theta} = 0.05$	$\delta_{\Theta} = 0.1$	$\delta_{\Theta} = 0.2$	Nominal
DI	1.38×10^{-3}	1.40×10^{-3}	1.44×10^{-3}	1.38×10^{-3}

Table 1. Comparison between DI obtained for the nominal model and the estimated values for the mean.

There is a correspondence between a crack depth, \bar{a} , and a DI for a given excitation (Fig. 4). Then a chosen \bar{a} leads to a value for DI so that three different crack depth were used to establish a threshold for the DI as the failure surface, Eq. 17: $\bar{a} = 0.16$, $\bar{a} = 0.17$ and $\bar{a} = 0.18$. Excitation shown at Fig. 2(a) and Fig. 2(b) are used leading to $DI = 0.00011$, $DI = 0.00016$ and $DI = 0.00021$ for 80 kHz and $DI = 0.00186$, $DI = 0.00245$ and $DI = 0.00319$ for 100 kHz. Note that \mathbf{X} is reduced to Θ . A coefficient of variation $\delta_{\Theta} = 0.1$ is chosen arbitrarily to perform the analysis. Convergence results are summarized in Fig. 6 for the Failure Probability, found after 20,000 Monte Carlo simulations, and results for both excitation frequencies were the same, so one of them was omitted.

For a $\bar{a} = 0.18$ threshold there were no failure events. The probability of a crack depth being bigger than $\bar{a} = 0.18$ is close to zero. For a $\bar{a} = 0.17$ the probability of failure is $PF = 0.085\%$ and for a $\bar{a} = 0.16$ the probability of failure is $PF = 6.87\%$. This analysis can be carried out for different dispersion parameters δ_{Θ} , meaning better (little δ_{Θ}) or worse (big δ_{Θ}) modeling.

Tab. 2 summarize this results. They can be analyzed in order to assess the robustness of uncertain crack model. The simulated cases show that, for a $\bar{a} = 0.15$ mean crack depth and $\delta_{\Theta} = 0.1$, the probability of the crack depth being bigger than $\bar{a} = 0.18$ is zero. It means the MC sampling was not able to simulate any trial for the crack depth bigger than $\bar{a} = 0.18$, so the failure probability is less than 1/20,000 (see, Eq. 19), not exactly zero.

	$\bar{a} = 0.16$	$\bar{a} = 0.17$	$\bar{a} = 0.18$
\hat{PF}	6.97×10^{-2}	8.50×10^{-4}	0.00

Table 2. Calculated \hat{PF} for the different strategies.

7. CONCLUDING REMARKS

In this paper a probabilistic modeling of the flexibility related to a crack in a rod has been presented. In this analysis only the flexibility of the crack has been considered uncertain. A wave propagation-based method, SEM, has been used to model the dynamic deterministic problem and the Castigliano's theorem and fracture mechanics theory have been used to associate a crack depth to a local flexibility. The uncertainties of the problem have been modeled with the probability theory together with the Maximum Entropy Principle, which allows to use only the available information to construct a probability distribution compatible with the physics of the problem.

The modeled flexibility can be considered uncertain due to the uncertainty associated to its parameters, and also to the

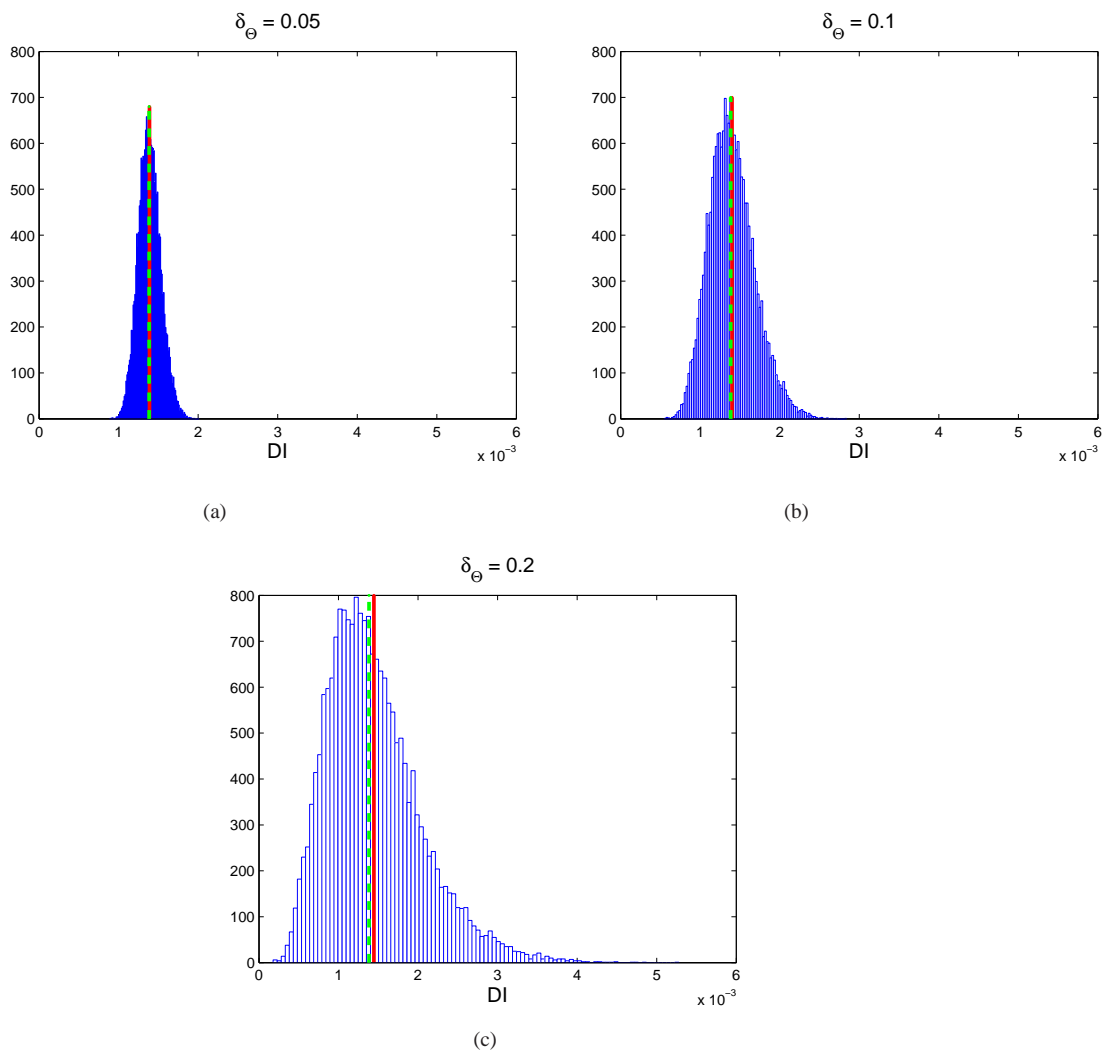


Figure 5. Histograms for DI using 20,000 MC simulation (a) $\delta_{\Theta} = 0.05$, (b) $\delta_{\Theta} = 0.1$ and (c) $\delta_{\Theta} = 0.2$. *DI* for nominal model is shown in green and *DI* mean is shown in red.

uncertainty associated to the own model. The dispersion parameters can be interpreted as better (little δ_{Θ}), or worse (big δ_{Θ}) modeling. For a given mean crack depth, $\underline{\theta}$, the influence of different coefficient of variation, δ_{Θ} , is analyzed using histograms for *DI* and results for estimated mean value of *DI* are compared to the value obtained using nominal values of the model.

An index *DI*, that compare the non-cracked structural behavior with the cracked behavior, has been used to quantify the damage related to the crack at a specific (deterministic) location. A burst is applied at one point of the rod and it is reflected at the crack location. This phenomenon is used to detect the damage. Better results are obtained to determine the damage location using the FRF at different points across the structure, as shown at Banerjee et al. (2009).

A reliability analysis was performed in order assess the robustness of the given crack model to predict a crack depth, increasing the prescribed limit threshold for the *DI* until no failure occur, given when $\bar{a} = 0.18$. For a given $\underline{\theta}$ and δ_{Θ} , this analysis gives the probability of a measured signal, here obtained by a simulation, be related to a crack depth. Different frequency of excitations are used to built the bursts and it is noted that the used *DI* is very sensitive to this, however it had no influence at the probability of failure to different thresholds. The simulated cases show that there is no probability of the crack depth being bigger than $\bar{a} = 0.18$ and that there is a little probability of the crack depth being bigger than $\bar{a} = 0.17$.

The direct MC sampling was used as the stochastic solver. It is a very expensive methodology, but the SEM approach to modeling a cracked rod minimize the computational efforts to perform the simulation. A complex 2×2 matrix is able to represent the problem, with the advantage of using the related analytical solution, well-suited with the wave propagation approach used at structural health monitoring.

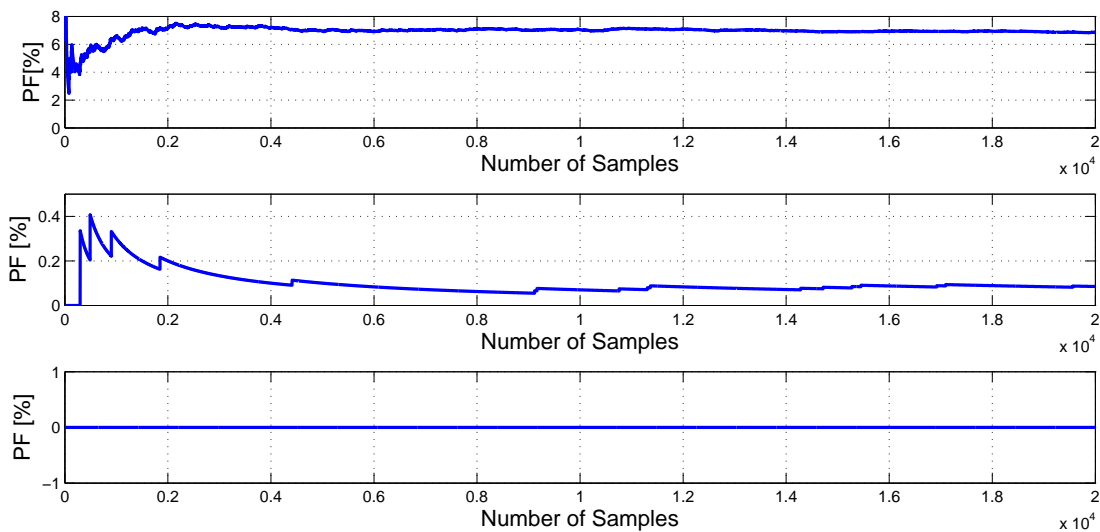


Figure 6. Probability of Failure convergence for different failure surface $\bar{\alpha} = 0.16$ (upper), $\bar{\alpha} = 0.17$ (middle) and $\bar{\alpha} = 0.18$ for both frequency excitations.

8. ACKNOWLEDGEMENTS

The authors acknowledge Tecumseh do Brasil for a graduate scholarship and the financial support of the Brazilian agencies CNPQ, FAPERJ, and CAPES (Projeto Pro-Engenharia 086/2008).

9. REFERENCES

- Arruda, J. R. F., Ahmed, K. M., Ichchou, M. N., Mencik, J. M., 2007. Investigating the relations between the wave finite element and spectral element methods using simple waveguides. In: Proceedings of COBEM 2007. Brasília, Brazil.
- Banerjee, S., Ricci, F., Monaco, E., Mal, A., 2009. A wave propagation and vibration-based approach for damage identification in structural components. *Journal of Sound and Vibration* 322, 167–183.
- Craig, R. R., 1981. *Structural Dynamics: An Introduction to Computer Methods*. John Wiley, New York.
- Doyle, J. F., 1997. *Wave Propagation in Structures*. Springer, New York.
- Haldar, A., Mahadevan, S., 2000. *Reliability Assessment Using Stochastic Finite Element Analysis*. John Wiley & Sons, USA.
- Jaynes, E., 1957a. Information theory and statistical mechanics. *The Physical Review* 106 (4), 1620–630.
- Jaynes, E., 1957b. Information theory and statistical mechanics II. *The Physical Review* 108, 171–190.
- Kapur, J. N., Kesavan, H. K., 1992. *Entropy Optimization Principles with Applications*. Academic Press, Inc., USA.
- Krawczuk, M., Grabowska, J., Palacz, M., 2006a. Longitudinal wave propagation. part I - comparison of rod theories. *Journal of Sound and Vibration* 295, 461–478.
- Krawczuk, M., Grabowska, J., Palacz, M., 2006b. Longitudinal wave propagation. part II - analysis of crack influence. *Journal of Sound and Vibration* 295, 479–490.
- Ostachowicz, W. M., 2008. Damage detection of structures using spectral finite element method. *Computers & Structures* 86, 454–462.
- Palacz, M., Krawczuk, M., 2002. Analysis of longitudinal wave propagation in a cracked rod by the spectral element method. *Computers & Structures* 80, 1809–1816.
- Pereira, F. N., 2009. Wave propagation and damage detection with high order rod models by the spectral element method. Master's thesis, University of Campinas, Campinas - SP, Brazil.
- Rackwitz, R., 1991. Reliability analysis - a review and some perspectives. *Structural Safety* 23, 297–331.
- Rubinstein, R. Y., Kroese, D. P., 2008. *Simulation and the Monte Carlo Method*. John Wiley & Sons, USA.
- Schuëller, G., 2007. On the treatment of uncertainties in structural mechanics and analysis. *Computers & Structures* 85, 235–243.
- Schuëller, G. I., 2001. Computational stochastic mechanics - recent advances. *Computers & Structures* 79, 2225–2234.
- Shannon, C. E., 1948. A mathematical theory of communication. *Bell System Tech. J.* 27, 379–423 and 623–659.
- Sudret, B., der Kiureghian, A., November 2000. Stochastic finite element methods and reliability: A state-of-the-art

report. Technical Report, University of California, Berkeley (UCB/SEMM-2000/08).

10. Responsibility notice

The authors are the only responsible for the printed material included in this paper